Science of the Total Environment 907 (2024) 167956

Contents lists available at ScienceDirect

Science of the Total Environment

journal homepage: www.elsevier.com/locate/scitotenv

Exposure to pentachlorophenol destructs the symbiotic relationship between zooxanthellae and host and induces pathema in coral *Porites lutea*

Yuanyuan Zhang [a,b], Lan Luo [a], Pin Gan [a], Xuan Chen [a], Xiaoli Li [a], Yan Pang [a], Xiaopeng Yu [a], Kefu Yu [a,b,*]

[a] School of Marine Sciences, Guangxi Laboratory on the Study of Coral Reefs in the South China Sea, Guangxi University, Nanning 530004, China
[b] Southern Marine Science and Engineering Guangdong Laboratory (Zhuhai), Zhuhai 519000, China

HIGHLIGHTS

- Exposure to pentachlorophenol will cause coral bleaching in *Porites lutea*.
- Increase of the pathogenic bacterium *Citrobacter* may be one of the bleaching inducers.
- The metabolism of amino acids and carbohydrates in zooxanthellae was abnormal.
- Upregulation of toxic differentially expressed metabolites led to coral pathema.

GRAPHICAL ABSTRACT

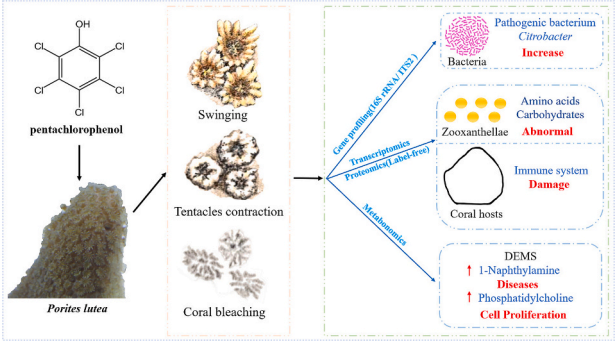

ARTICLE INFO

Editor: Julian Blasco

Keywords:
Coral bleaching
Pentachlorophenol
Symbiotic relationship
Citrobacter
Coral pathema

ABSTRACT

Stress from chemical pollutants is among the key issues that have adverse impacts on coral reefs. As a persistent organic pollutant, pentachlorophenol (PCP) has been detected in the seawater of Weizhou Island and was proved to have significant adverse effects on aquatic animals. However, little is known about its effects on scleractinian coral. Therefore, we investigated the response of the coral *Porites lutea* to PCP stress. Coral bleaching, photosynthesis parameters and antioxidant enzyme activities of *P. lutea* under PCP exposure were documented. After 96 h of exposure, significant tissue loss and bleaching occurred when the PCP concentration exceeded 100 μg/L. The density of symbiotic zooxanthellae decreased from 2.06×10^6 cells/cm^2 to 0.93×10^6 cells/cm^2 when the PCP concentration increased from 1 μg/L- 1000 μg/L. Long-term exposure of 120 days to PCP at 0.1 μg/L also led to coral bleaching, the maximum photochemical quantum yield of PSII in *P. lutea* nubbins significantly decreased to 0.482. The analysis of microbial community distribution indicated that the increase of the pathogenic bacterium *Citrobacter* may be one of the inducers of coral bleaching. Conjoint analysis of transcriptomics and proteomics showed that the metabolism of amino acids and carbohydrates in zooxanthellae was abnormal, leading to the destruction of its symbiotic relationship with the host. The immune system of the host was disrupted, which could be linked to the prevalence of coral pathema. The toxic responses of PCP on both zooxanthellae and

* Corresponding author at: School of Marine Sciences, Guangxi Laboratory on the Study of Coral Reefs in the South China Sea, Guangxi University, Nanning 530004, China.
E-mail address: kefuyu@scsio.ac.cn (K. Yu).

https://doi.org/10.1016/j.scitotenv.2023.167956
Received 8 August 2023; Received in revised form 17 October 2023; Accepted 18 October 2023
Available online 24 October 2023

its host were further confirmed by the upregulation of the differential metabolites including 1-naphthylamine and phosphatidylcholine, etc.

1. Introduction

Despite covering only a small fraction (<0.1 %) of the Earth's surface, coral reefs are among the most bio-diverse ecosystems on earth (Thatje, 2021). The ecosystem not only provides foods and financial incomes to people but also serves as a barrier against natural hazards (Corinaldesi et al., 2018). Unfortunately, due to a number of environmental impacts, coral reefs worldwide are facing degradation (Ding et al., 2019). One of the most pressing issues is global climate change, which disrupts the symbiotic relationship between corals and zooxanthellae when corals are exposed to rising sea temperatures (Wright et al., 2019; Yu et al., 2020). Additionally, the threat of chemical pollution to coral reefs is becoming increasingly concerning as the rate of chemical pollution is much faster than that of global warming (Han et al., 2020).

Recently, it has been demonstrated that some chemical pollutants can induce coral bleaching through the loss of symbiotic zooxanthellae within corals (Corinaldesi et al., 2018; Feng et al., 2020; He et al., 2019). This results in the loss of photosynthesis and a decrease in energy, making it difficult for corals to survive in a bleached state (Pernice and Hughes, 2019; Sun et al., 2023). As a potential indicator of environmental stress, coral bleaching has been identified (Shlesinger and van Woesik, 2023). The impact of chemical compounds contained in sunscreens and other personal care products on coral has been frequently studied (Fel et al., 2018; McCoshum et al., 2016; Raffa et al., 2019). Heavy metals particularly copper and microplastics have been recognized as significant stressors for coral reefs (Reichert et al., 2018; Schwarz et al., 2013). Besides, agriculture pollutants such as pesticides, herbicides and crude oil products have also been reported to pose a threat to coastal coral reef ecosystems (Lewis et al., 2016; Nahar et al., 2023). Wecker et al. reported the exposure to chlordecone induced detoxification genes and caused polyp bail-out in the coral *Pocillopora damicornis* (Wecker et al., 2018). However, there is little research on the toxic effects of chlorophenol pollutants on corals.

Light industries such as paper making, textile printing and dyeing, and wood processing are mostly located in coastal areas in China to facilitate the transportation of raw materials and products. It is inevitable that the chemical pollutants generated in the production process will be discharged into the sea. Pentachlorophenol (PCP) is a persistent organic pollutant that is widely used in these industries to prevent termites and wood decay (Kobusińska et al., 2016; Lewandowski et al., 2018). It was reported to be one of the main contributors to the ecological risk in the seawater and estuarine water samples from the semiclosed Bohai Sea with residue concentrations as high as 530 ng/L (Feng et al., 2022). PCP is also easily adsorbed by marine organisms and persists for a long time due to its high octanol-water distribution coefficient ($\log_{Kow}$ = 5.12) (Kobusińska et al., 2016). For instance, the concentration of PCP was detected to be 0.16–9.06 μg/kg in mud crab from Hangzhou Bay, China (Zheng et al., 2018). Due to its persistent ecological risks, PCP is regulated under the Stockholm Convention on Persistent Organic Pollutants (Lewandowski et al., 2018). However, its persistent ecological risks to the marine ecosystem should be continuously monitored, as it is still used as a timber preservative (Beiras and Tato, 2018). PCP was reported to have a strong inhibitory effect on the respiration and metabolism, causing oxidative damage to liver and other organs in aquatic animals (Zheng et al., 2011). It was proved that PCP had significant adverse effects on hematopoietic and immune system development in zebrafish. PCP exposure may affect the timing and coordination of central nervous system development of zebrafish, and change the level of thyroid hormone by interfering with the regulatory pathway of thyroid hormone (Cheng et al., 2015; Namit et al., 2022).

Transcriptomics, proteomics and metabolomics have been widely applied in coral research to reveal the response of coral organisms under various environmental pressures (Yu et al., 2021a; Yu et al., 2021b). However, life activities are complex, analysis of only a single omic layer is limited. Integration of various omics is often used to elucidate potential causative changes that lead to a disease or identify the treatment targets, which can be tested in subsequent molecular studies (Toonen et al., 2018). At present, it is rare to use conjoint analysis of transcriptome, proteome and metabolomics to analyze the mechanism of coral's influence on exogenous pollutant stress. The toxic mechanisms at the cellular and molecular levels of PCP on coral reefs are still scarce and worth investigating.

The Beibu Gulf located in the northern part of the South China Sea is a semi-closed bay and experiencing limited water exchange (Ma et al., 2022). The coastal industries in the provinces of Guangxi, Guangdong, and Hainan have led to a buildup of chemical pollutants in the seawater and marine ecosystems. Weizhou Island located in the middle of the Beibu Gulf is home to high-latitude marginal reefs (Yu et al., 2019). Over the past 30 years, the coral reef ecosystem of the island declined significantly (Chen et al., 2013). We have detected PCP with a concentration of 10 ng/L − 100 ng/L in the seawater of Weizhou Island. In this study, we examined the toxicity effects and mechanisms of PCP on the widely distributed coral species *Porites lutea* in Weizhou Island in the following ways: (1) investigate the impact of PCP on *P. lutea* bleaching through the apparent morphological change and quantify the toxic effects of PCP on *P. lutea* using parameters such as zooxanthellae density, maximum photochemical quantum yield of photosystem II (PSII), chlorophyll *a* content, and antioxidant enzyme activities, (2) test the community changes in symbiotic bacterial and zooxanthellae under PCP exposure, (3) analyze the mechanisms of PCP-induced damage in symbiotic zooxanthellae and host of *P. lutea* at the cellular and molecular levels from multiple omics including transcriptomics, proteomics and metabolomics. This study provides new clues for understanding the physiological response of coral to environmental stress and pathogen infection.

2. Materials and methods

2.1. Chemicals

A chemical standard for PCP was obtained from the National Institute of Metrology. Methanol was used to dissolve PCP at a concentration of 1.01 mg/mL. The commercial kits of superoxide dismutase (SOD) and catalase (CAT) assay in the supernatants were obtained from Nanjing Jiancheng Bioengineering Institute, Nanjing, China. The BCA protein assay kit was purchased from Sangon Biotech, Shanghai, China.

2.2. Coral collection and culture

The *P. lutea* coral colonies of were collected from the reef in Weizhou Island, Guangxi, China and transported to the Guangxi Laboratory on the Study of Coral Reefs in the South China Sea, where several species of coral colonies including *P. lutea* have been cultivated for >8 years. The colonies were acclimated to new conditions for 60 days in a flow-through aquarium (60 cm × 60 cm × 60 cm) with a temperature of 26 °C and a flow rate of 3 L/min using artificial seawater. A 12:12 h light/dark cycle was provided using an aquarium light (250 W metal halogen lamp and 4 T5HO) that mimicked natural light. Water quality parameters are listed in the supplementary material (Table S1). In order to ensure the consistency of the experiment, nubbins from the same mother colony were used for the same set of experimental data. We cut the cultured coral colonies into small nubbins (2–4 cm long) and

distributed them equally in the coral tanks. The nubbins were acclimated to tank conditions for >30 days before the start of the PCP exposure experiment.

2.3. PCP exposure assay

Healthy coral nubbins with fully healed wounds were then transferred to 15-l glass tank for a period of at least 14 days. The water quality, flow rate, and temperature in the bottles were kept consistent with those in the coral tank. The selected coral nubbins were characterized by polyps that were sensitive to touch and reopened within 1 min, dark-colored external tissues, and a pure white skeleton. In a fully controlled laboratory experiment, these nubbins were exposed to PCP at concentrations ranging from 1 to 1000 μg/L over 24 to 96 h (Watanabe et al., 2006). The concentration of PCP was selected based on its biotoxicity to zebrafish, a commonly used model for biotoxicity testing of chemical substances (Cheng et al., 2015; Namit et al., 2022). Due to the low concentration of PCP in the actual environment, we conducted a long-term exposure experiment with 0.1 μg/L PCP. Simultaneous blank and solvent controls (0.01 % methanol) were conducted, and at least three replicates were prepared for each exposure.

2.4. Apparent morphological change of P. lutea

For comparison, the corals were continuously monitored throughout the exposure experiment. Visible tissue loss and bleaching were documented using an Olympus Tough TG-5 camera under consistent lighting conditions (the same time every day, under the same lighting, and at the same angle). The digital photographs were analyzed by photo editing software (Adobe Photoshop) to determine the color composition (CMYK, cyan, magenta, yellow, and black) (Danovaro et al., 2008). Image-Pro Plus (version 6.0) was utilized to quantify the levels of coral bleaching by comparing the color of the corals before and after PCP treatment (Chow et al., 2016; Huang et al., 2022).

2.5. Quantification of P. lutea responses to PCP

The maximum photochemical quantum yield (Fv/Fm) of *P. lutea* was determined by pulse amplitude modulation fluorometry (Diving-PAM). Fv/Fm serves as a reliable approximation for the maximum photochemical efficiency of photosystem II (PSII). To ensure accurate measurements, the corals were dark-adapted for 30 min, allowing them sufficient time to acclimate (Schreiber, 1986). Three measurements were taken for each coral nubbin using a Diving-PAM fluorometer (Walz, Germany) in complete darkness, on each experimental day (Huang et al., 2022).

The density of zooxanthellae in *P. lutea* was calculated by dividing the number of zooxanthellae by the surface area of coral tissue and expressing it as 10^6 cells/cm^2 (Drew, 1972; Nakamura et al., 2004). Coral fragments to be tested were washed by a recirculating Waterpik containing filtered seawater. The washing solution was then isolated by gradient centrifugation. The precipitates were collected after centrifugation at 6000 rpm for 5 min, and the supernatants were used to assess the antioxidant enzymes, including SOD and CAT activities by commercial kits (Higuchi et al., 2008). Then, the precipitates were resuspended in filtered seawater and centrifuged again at 4000 rpm for 5 min. The number of zooxanthellae was counted using a microscope (Olympus, Japan) and a hemocytometer plate, while the surface area of the coral tissue was measured using the tin foil method (Qin et al., 2019).

The chlorophyll *a* content served as a reliable indicator for assessing the physiological condition of zooxanthellae. It is measured by the concentration of chlorophyll *a* in a specific area, typically expressed μg/cm^2. After centrifuging at 4000 rpm for 5 min, the solution containing bacterial cells was precipitated at 4 °C and extracted with 90 % acetone, ensuring protection from light, for a period of 24 h. Then, the mixture was centrifuged at 4000 rpm again for 5 min, the supernatant was collected, and the absorbance was measured at 630, 647, 664 and 750 nm. The concentration of chlorophyll *a* in the zooxanthellae was calculated according to the formula (Huang et al., 2022):

$$(\text{chl a} = 11.85 \times (\text{A664} - \text{A750}) - 1.54 \times (\text{A647} - \text{A750}) - 0.08 \times (\text{A630} - \text{A750}) \times \text{V}/\text{S}$$

where V represents the initial sizing volume, S represents the surface area which is determined by analyzing the relationship between the weight of the foil and its surface area (Ritchie, 2006; Xiang et al., 2019).

2.6. Biomics analysis

In the analysis of microbial diversity (Text S1), high-throughput sequencing technology was employed to assess the diversity of Symbiodiniaceae and bacteria in corals (Silva et al., 2022). Genomic DNA extracted from the symbiotic family and bacteria was amplified using the ITS2 sequence and 16S rRNA sequence, respectively (Chen et al., 2021; Cunning et al., 2017). The sequencing was conducted on the Illumina MiSeq platform. Taxonomic analysis of the denoised sequences (ASVs) obtained through DADA2 was carried out using the classifier in Quantitative Study of Microbial Ecology 2 (QIIME2) (Xu et al., 2023; Zhang et al., 2021).

In transcriptomics analysis (Text S2), total RNA was extracted from the coral using Trizol reagent (Invitrogen, Carlsbad, CA, USA). Subsequently, the quality and quantity of the extracted RNA were assessed. The mRNA isolated with oligo (dT) was fragmented using a fragmentation buffer. Random primers were then used to convert the mRNA fragments into cDNA. Following cDNA terminal repair, the enriched library was sequenced using the Illumina NovaSeq 6000 platform. All sequencing was performed at Majorbio Biopharm Technology Co., Ltd. Transcriptome assembly, differential expression analysis, and functional enrichment were conducted subsequent to sequencing and sequence alignment (Helmkampf et al., 2019; Jiang et al., 2022; Li et al., 2020a; Yoshioka et al., 2021).

In the 4D label-free proteomics analysis (Text S3), we determined the concentration of proteins isolated from coral tissue and evaluated the quality of the samples. After enzymatic digestion of the proteins, the peptide fragments were extracted, desalted using HLB, and then vacuum dried. The peptide concentrations were determined using the peptide quantification kit (Thermo, Cat. 23275). Equal amounts of the samples were subjected to LC-MS/MS analysis, and the resulting MS/MS spectra were searched against a database using MaxQuant version 2.0.3.1 software. The search results were further analyzed both statistically and bioinformatically (Pei et al., 2023; Pei et al., 2022b).

In the metabolomics analysis (Text S4), samples underwent metabolite extraction first, followed by injection into the UHPLC-Q Exactive HF-X system by Thermo Fisher Scientific for LC-MS/MS analysis. The raw data from LC/MS was imported into the metabonomics processing software Progenesis QI (Waters Corporation, Milford, USA). The identification of metabolites was performed by searching against a database, which was uploaded to the Majorbio cloud platform (cloud.majorbio.com) for data analysis (Lohr et al., 2019; Pei et al., 2022a).

2.7. Statistical analysis

All physiological data were presented as mean ± standard deviation (SD). Statistical significance of differences was assessed through analysis of variance (ANOVA) followed by multiple comparisons (S-N-K). The above statistical analysis was performed with SPSS (IBM, Statistics 26, USA) and the significant differences were defined as $p < 0.05$.

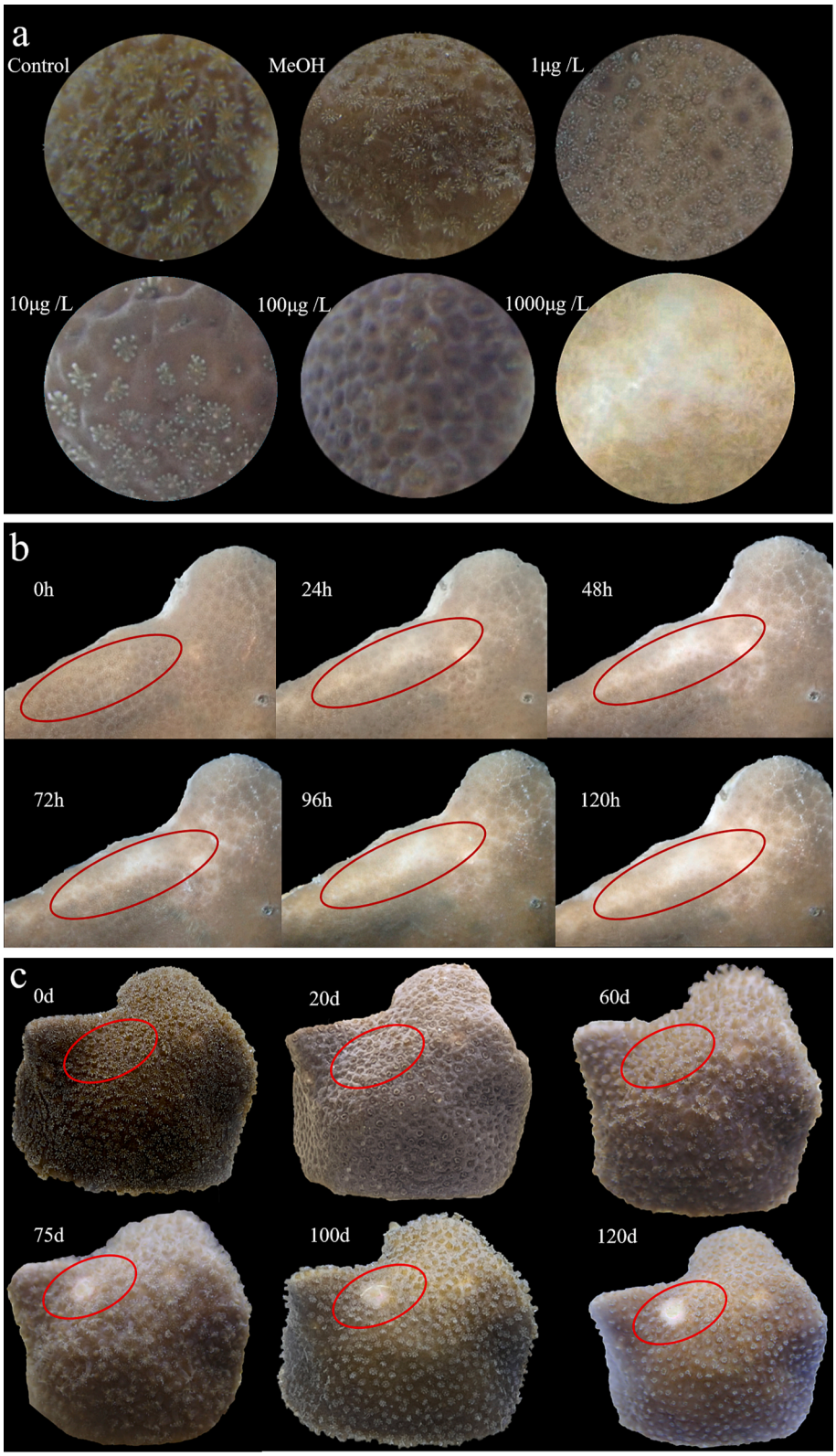

Fig. 1. Images of *P. lutea* phenotype. (a) Representative photographs of *P. lutea* fragments exposed to different concentrations of PCP for 96 h; (b) Representative photographs of *P. lutea* fragments exposed to different times of 1000 μg /L PCP; (c) Representative photographs of *P. lutea* fragments exposed to different times of long-term exposure to low concentration PCP.

3. Results and discussion

3.1. Coral bleaching, photosynthesis parameters and antioxidant enzyme activities of P. lutea under PCP exposure

The blank and solvent control nubbins showed minimal changes throughout the experiment, while the nubbins exposed to PCP solutions at concentrations of 1 μg/L- 1000 μg/L for 96 h displayed varying levels of tissue loss and bleaching. As shown in Fig. 1a, some tentacles contracted slightly at concentration of 1 μg/L, but most of the tentacles were still extending. When the PCP concentration increased to 10 μg/L, the proportion of the contracted tentacles increased. Significant tissue loss and bleaching occurred when the PCP concentration exceeded 100 μg/L. Under exposure to PCP at a concentration of 1000 μg/L, as the exposure time increased, corals began to experience tentacle contraction or even bleaching (Fig. 1b). To quantify the levels of coral bleaching, the shifts in the relative proportions of different color components on digital photographs of *P. lutea* were also analyzed. As shown in table S2, the shift between the coral's color components including cyan, magenta, yellow and black (CMYK) increased with the increase of PCP stress time. Similar color shifts of hard corals were observed during the exposure experiments of sunscreen and sunscreen ingredients (Danovaro et al., 2008). This is manifested at the colony level as a dramatic loss of the brown pigment of the symbiotic dinoflagellate from coral colonies (coral bleaching) (Rosic Nedeljka et al., 2010). The high concentrations were selected in an attempt to better understand the stress effects of *P. lutea* after exposure to PCP. However, the concentration of PCP in the actual environment is very low. As shown in Fig. 1c, under long-term exposure for 4 months at a low concentration of 0.1 μg/L PCP, coral tentacles severely contracted at 20 days. Additionally, corals exhibited significant tissue loss and bleaching at 75 days, and the effects were more pronounced at 120 days.

The change of the density of symbiotic zooxanthellae is consistent with the levels of coral bleaching (Fig. 2a). There was no significant change between the blank and the solvent control group ($p > 0.05$), which was 2.65×10^6 cells/cm^2 and 2.56×10^6 cells/cm^2, respectively. The density significantly decreased to 2.06×10^6 cells/cm^2, 1.81×10^6 cells/cm^2, 1.19×10^6 cells/cm^2 and 0.93×10^6 cells/cm^2 at the PCP concentration of 1 μg/L- 1000 μg/L, respectively. It was also found that the maximum photochemical quantum yield of PSII in *P. lutea* nubbins significantly decreased with the increase of PCP concentrations ($p < 0.05$, Fig. 2b). As reported, the breakdown of the symbiosis between corals and their dinoflagellates began with photosynthetic dysfunction due to damage to PSII (Takahashi and Murata, 2008). It was also found that the maximum photochemical quantum yield of PSII in *P. lutea* nubbins significantly decreased to 0.482 with the increase of PCP exposure time during the long-term exposure for 4 months at a low PCP concentration of 0.1 μg/L (Fig. S1).

A similar trend was observed in the decline of chlorophyll *a* content (Fig. 2c). With the increase of pentachlorophenol exposure

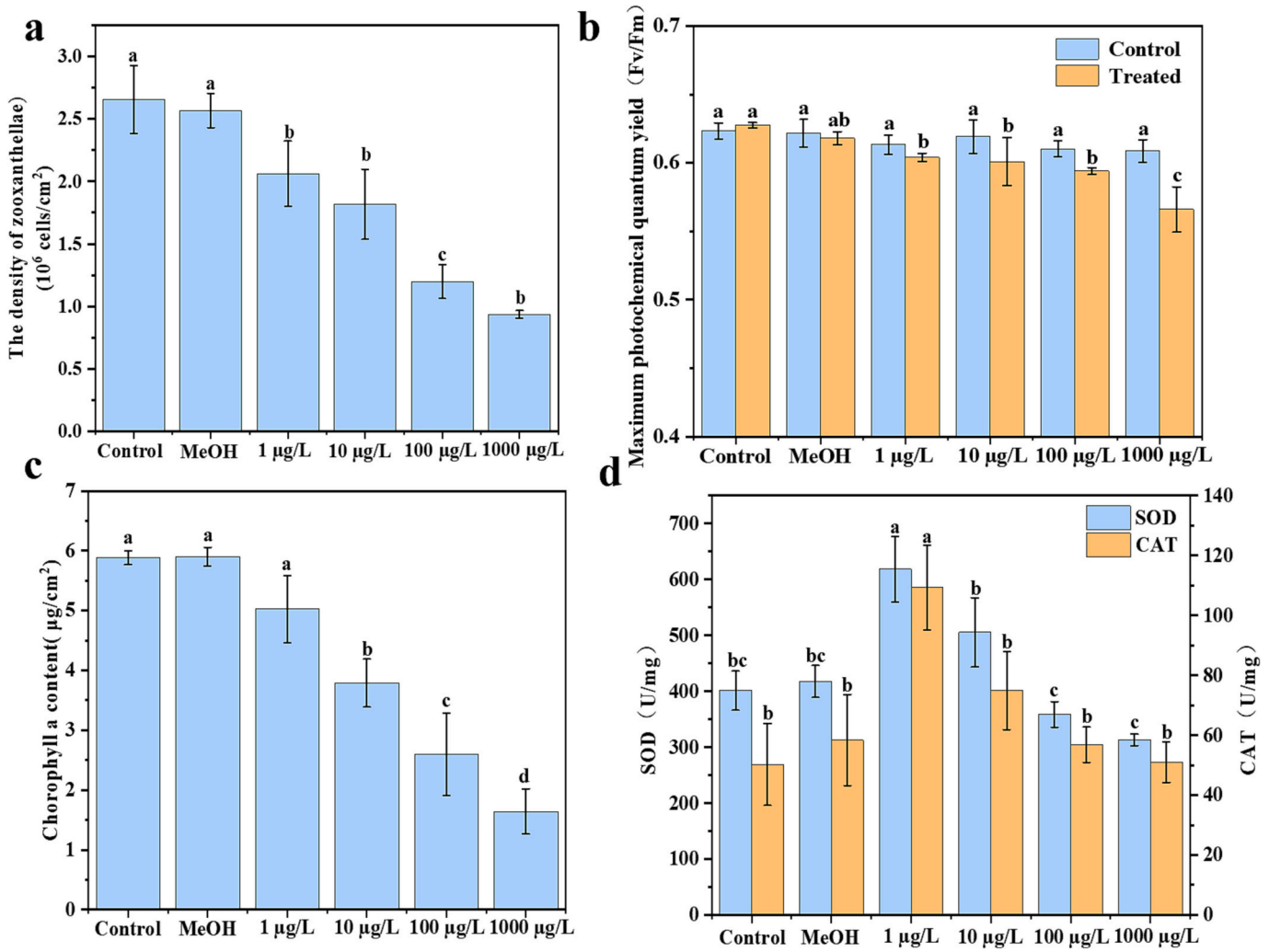

Fig. 2. Stress response of *P. lutea* under PCP exposure at various concentrations. (a) Density of symbiotic zooxanthellae; (b) Maximum photochemical quantum yield of PSII in *P. lutea*, (c) Chlorophyll a content; (d) CAT and SOD activities.

concentration, the content of chlorophyll-a in coral reefs gradually decreased. When the concentration of PCP was as high as 1000 μg/L, the chlorophyll *a* content was only 1.64 μg/cm^2, which was <30 % of the untreated blank nubbins. These results suggested that PCP can cause hard-coral bleaching by destabilizing the symbiosis between corals and their dinoflagellate symbionts, leading to loss of the symbionts from the tissues of the coral hosts (Weis, 2008).

The initiation of the antioxidant enzyme system can be considered the organism's response to resist environmental pollution and mitigate toxic damage (Cheng et al., 2021). Exogenous chemicals were reported to induce the expression of coral antioxidant enzymes (Tang et al., 2018). PCP could also alter the activity of antioxidant enzymes such as superoxide dismutase (SOD) and catalase (CAT) of organisms (Jiang et al., 2017; Michałowicz et al., 2009). As shown in Fig. 2d, there was no significant change in the CAT and SOD in the blank and the solvent control group. When exposed to 1 μg/L of PCP, CAT and SOD activities significantly increased to 109.3 U/mg and 618.7 U/mg, respectively. However, as the concentration of PCP increased to above 10 μg/L, the CAT and SOD activities decreased. The phenomenon is consistent with the stress response of the coral *P. damicornis* under exposure to chlordecone (Wecker et al., 2018). The reason may be attributed to that under exposure to lower concentrations of PCP, the antioxidant enzyme activities of *P. lutea* cells were promoted to resist environmental stress, but higher concentrations of PCP exceeded the load of *P. lutea* stress system and destroyed its defense function (Zhang et al., 2023).

3.2. Community changes in symbiotic bacterial under PCP exposure

Many studies have confirmed the presence of a dynamic microbiota in both the coral surface mucus layer and tissue, indicating the crucial role bacteria play in coral health (Liang et al., 2022). We conducted an analysis of changes in the community composition of coral symbiotic bacteria after exposure to PCP. To address the potential impact of sequencing depth, we rarefied the number of sequences from the 16S rRNA region to 24,299, resulting in an average Good's coverage of 70 %. Taxonomic classification of ASVs was performed using the Naive Bayes consensus taxonomy classifier. Microbial community similarity at the family level was evaluated by PCoA based on Bray-Curtis distances. PCoA resulted in a 2-dimensional solution in which PC1 and PC2 accounted for 34.30 % and 20.41 % of the variation, respectively (Fig. S2). Overall, results indicated a clear division between the coral compartments exposed to different treatments (Yu et al., 2020). The microbial diversity in coral communities at the phylum, class, order, family, and genus levels did not significantly change in response to PCP

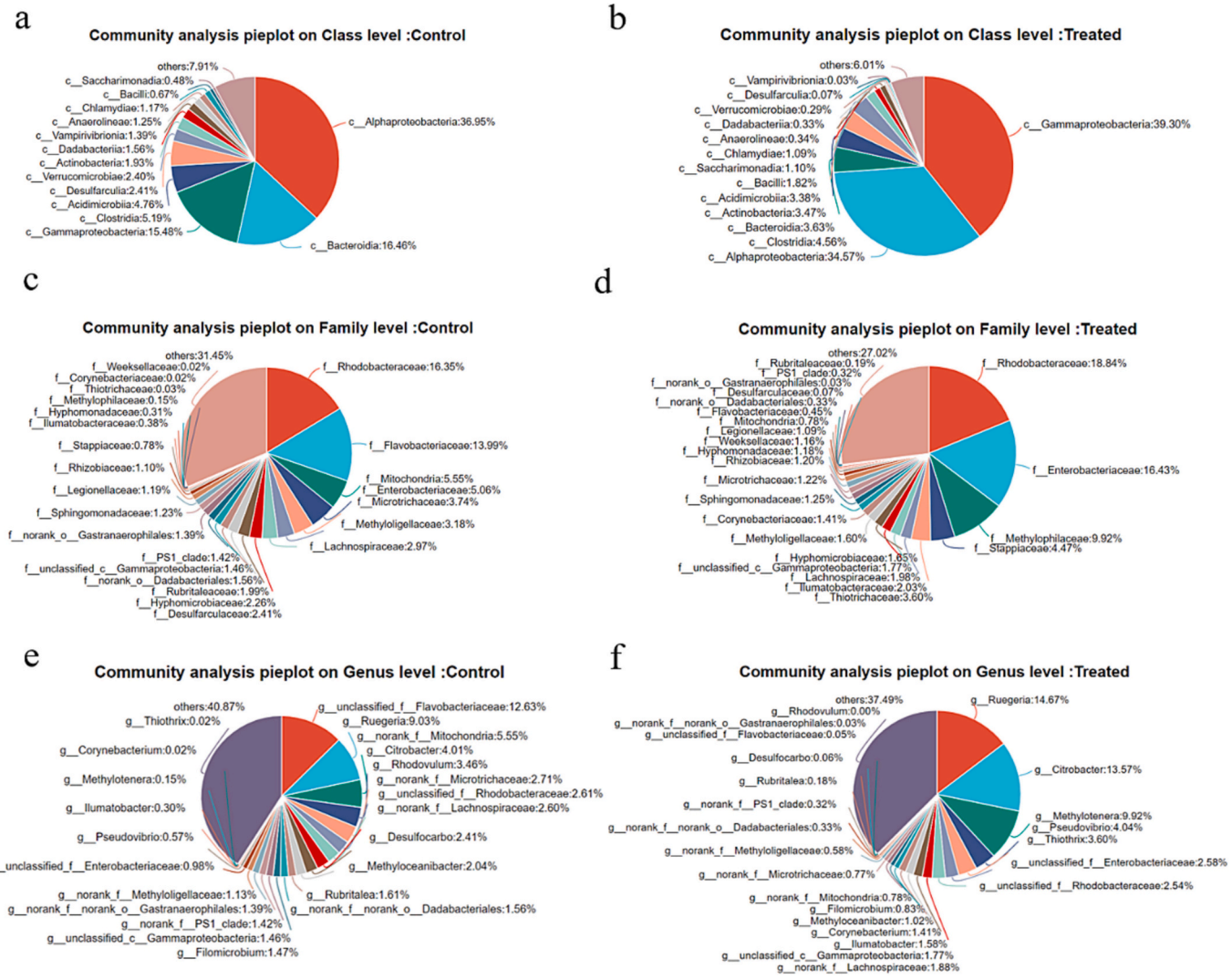

Fig. 3. Analysis of the coralline symbiotic bacterial community. (a, b) Pie chart for analysis of community structure composition of symbiotic bacteria at class level of control and treated group; (c, d) Pie chart for analysis of community structure composition of symbiotic bacteria at family level of control and treated group; (e, f) Pie chart for analysis of community structure composition of symbiotic bacteria at genus level of control and treated group.

stress (table. S3). The first dominant core bacteria remained mostly consistent, with *Proteobacteria*, *Rhodobacterales*, *Rhodobacteraceae*, *Ruegeria* as the corresponding dominant bacteria, and the dominant class of bacteria changed from *Alphaproteobacteria* to *Gammaproteobacteria*. However, their proportions were significantly altered, indicating that PCP affected the composition of coral bacterial communities. The second dominant phylum shifted from *Bacteroidetes* to *Actinobacteria*, the second dominant class shifted from *Bacteroidia* to *Alphaproteobacteria* (Fig. 3a and b), the second dominant order shifted from *Flavobacteriales* to *Enterobacterales*, and the second dominant family shifted from *Flavobacteriaceae* to *Enterobacteriaceae* (Fig. 3c and d), which mostly consist of pathogenic bacteria (Ahasan et al., 2017).

As shown in Fig. 4, Circos analysis was used to visualize the corresponding abundance relationship between samples and bacterial communities at the genus level, confirming the results shown in the pie chart. At the genus level, *Ruegeria* was the dominant bacteria in both the control and experimental groups, accounting for 9.03 % and 14.67 %, respectively. The relative abundance of facultative anaerobic bacteria *Methylotenera* increased from 0.15 % to 9.92 % (Fig. 3e and f), possibly due to a decrease in symbiotic zooxanthellae density and photosynthetic rate under PCP stress, leading to a decrease in coral microecological oxygen concentration and ultimately an increase in the relative abundance of anaerobic bacteria. It is noteworthy that the relative abundance of the pathogenic bacterium *Citrobacter* increased from 4.01 % to 13.57 % after PCP stress. *Citrobacter*, especially *Citrobacter freundii* and *Citrobacter koseri*, produce beta-lactamases that can hydrolyze the beta-lactam ring, similar to *Escherichia coli*, *Klebsiella pneumoniae*, and *Proteus* spp., thereby disrupting the host's defense against harmful bacteria (Ahasan et al., 2017). In animal studies, related research has shown that *C. freundii* can cause sepsis, a life-threatening organ dysfunction caused by the host's dysregulated response to infection. Furthermore, research has shown that *C. freundii* infection in rats can induce colonic proliferative changes, which ultimately lead to colon cancer (Hess et al., 2004). Therefore, the increase of the pathogenic bacterium *Citrobacter* is one of the main stress responses of corals to PCP stress and may also be one of the inducers of coral bleaching.

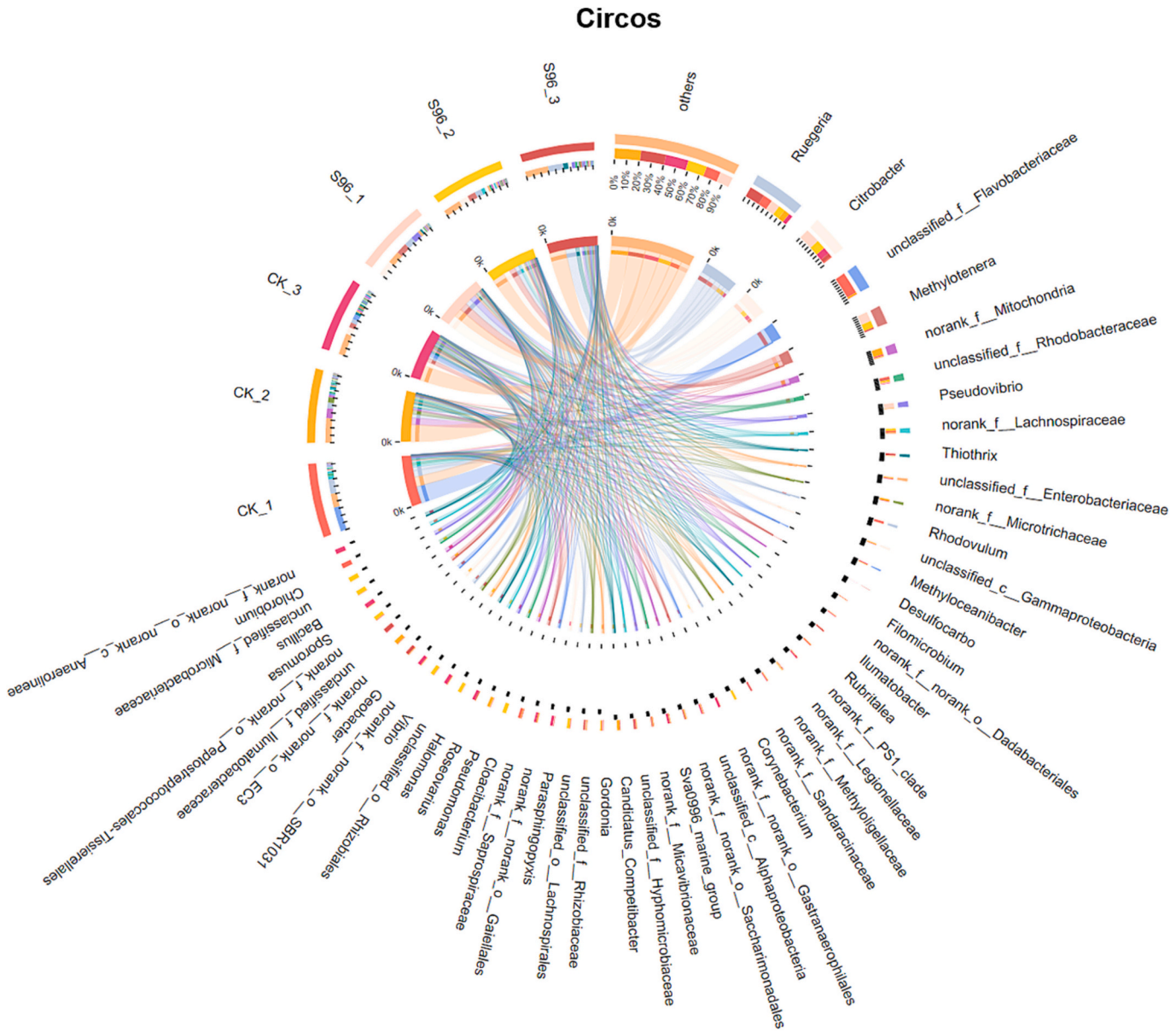

Fig. 4. Circos analysis of microbial community distribution at the genus level.

3.3. Response of symbiotic zooxanthellae under PCP exposure

The communities of the symbiotic zooxanthellae of *P. lutea* nubbins under PCP exposure were analyzed. As shown in Fig. S3, the main subclades in the zooxanthellae community structure remained relatively stable, and there was no significant difference in the ASV richness of symbiotic zooxanthellae between the control and experimental groups. Clade C15 was the most predominant subclade type in both groups with an average relative abundance of approximately 95.82 %. The dominance of the C lineage in the community structure of *P. lutea* may be attributed to the fact that the sample was collected from Weizhou Island in Guangxi, located in the northwest region of the South China Sea (SCS). Previous studies have reported that the C15 sub-lineage is the dominant lineage of *P. lutea* in the coral reef areas of the SCS (Huang et al., 2022). The reason why exposure of PCP did not alter the community structure of the symbiotic zooxanthellae of *P. lutea* may be attributed to the stable symbiotic relationship between the zooxanthellae and the coral host. Generally, the community structure of zooxanthellae is the result of long-term natural selection and coevolution. The variation in Symbiodiniaceae community structure was associated with the shift in the latitudinal gradient and varied significantly among coral species (Qin et al., 2019). Symbiodiniaceae communities are affected by the combined effects of environmental and geographic variables (Chen et al., 2021; De Palmas et al., 2015). The stress duration of this experiment was only 96 h, which was insufficient to produce a significant impact on the community structure of the symbiotic zooxanthellae (Yu et al., 2020). Further research is needed to determine whether long-term PCP stress would alter the symbiotic zooxanthellae structure of *P. lutea*. However, the stability of zooxanthellae does not imply their lack of involvement in the response to PCP stress. On the contrary, as an important component of the coral symbiotic functional unit, zooxanthellae are direct participants in the response of the coral symbiotic unit to environmental stress, and play an important role in maintaining the stability of the unit. Therefore, biomics analysis on zooxanthellae at gene and protein levels were conducted conjoint. Transcriptomic and proteomic analyses of zooxanthella including Venn analysis of transcriptomic, correlation heat map of proteomic samples, differential gene and protein volcano map and

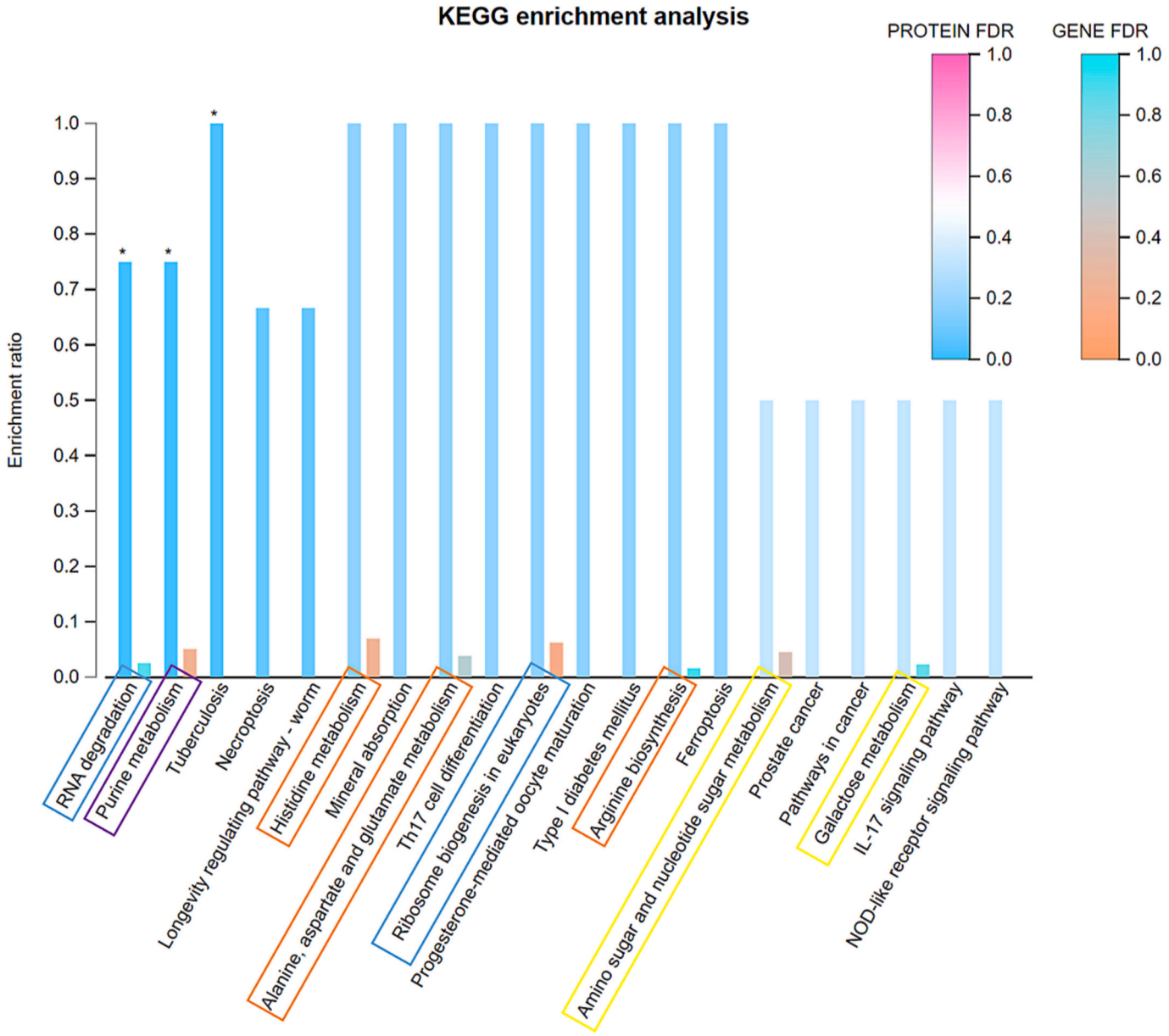

Fig. 5. Conjoint analysis of differentially expressed genes and proteins in the KEGG pathway of zooxanthellae.

differential gene and protein KEGG pathway enrichment analysis were shown in Fig. S4.

As shown in Fig. 5 and Table S4, the KEGG pathways that involved both 35 differentially expressed genes (DEGs) and 12 differentially expressed proteins (DEPs) include: (1) Metabolic pathways, such as amino acid metabolism-related pathways including alanine, aspartate, and glutamate metabolism, arginine biosynthesis, and histidine metabolism, nucleotide metabolism-related pathways such as purine metabolism, carbohydrate metabolism-related pathways, such as amino sugar and nucleotide sugar metabolism, and galactose metabolism. (2) Genetic information processing pathways, such as RNA degradation, ribosome biogenesis in eukaryotes. Nucleotides participate in fundamental biological activities such as inheritance, development, and growth. Purine synthesis is the process of synthesizing purine nucleotides in organisms, and various amino acids play important roles in this process (Singh and Anand, 2023). For example, aspartate is a substrate for the first key enzyme ATP phosphotransferase in the purine synthesis pathway and is one of the amino acids involved in the early stages of purine nucleotide synthesis. Glutamate, alanine, histidine, and other amino acids also participate in different steps of purine synthesis, playing regulatory and catalytic roles. Abnormalities in amino acid metabolism led to abnormalities in purine metabolism, disrupting nucleotide metabolism and preventing symbiotic zooxanthellae from carrying out normal life activities (Zhang et al., 2022). It has been reported that *Ictalurus punctatus* exposed to phenol experienced a decrease in plasmatic concentrations of amino acids. Sublethal concentrations of phenol can lead to an increase in carbohydrates of *I. punctatus* (Moraes et al., 2016). In rat intestines, PCP treatment suppressed carbohydrate metabolism, inhibited enzymes in the brush border membrane (BBM) of the intestine, and caused abnormal amino acid transport (Maheshwari et al., 2022). The main function of zooxanthellae is to provide sufficient amino acids and various carbohydrates to the coral host through photosynthesis. Therefore, abnormalities in amino acid and carbohydrate metabolism disrupted the symbiotic relationship between the zooxanthellae and the host which was one of the main response mechanisms for *P. lutea* to PCP exposure. Rapid changes in the external environment were proved to destabilize the symbiosis between corals and their dinoflagellate symbionts, leading to loss of the symbionts from the tissues of the coral hosts (Rosic Nedeljka et al., 2010).

3.4. Response of coral host under PCP exposure

The response of *P. lutea* host under PCP exposure was analyzed by transcriptome and proteomics simultaneously. Transcriptomic and proteomic analyses of coral host including Venn analysis of transcriptomic, correlation heat map of proteomic samples, differential gene and protein volcano map and differential gene and protein KEGG pathway enrichment analysis were shown in Fig. S5.

As shown in Fig. 6 and Table S5, we obtained 4 branches containing 100 DEGs and 69 DEPs in 20 known KEGG pathways. Among them, metabolism, organismal system and environmental information processing consisted of 10, 6 and 2 pathways, respectively. As the destruction of the symbiotic relationship with zooxanthellae, abnormal energy and material metabolism occurred in the coral host. Notably, most of the gene expressions were up-regulated in the pathway related to exogenous chemicals metabolism such as metabolism of xenobiotics by cytochrome P450 (CYP450), glutathione metabolism and drug metabolism. CYP450 and glutathione-S-transferase (GST) are both cellular biomarkers which can serve as diagnostic tools to indicate variations in the physiological condition of an organism in response to environmental change (Rougée et al., 2006). Many aquatic invertebrates were reported to respond to xenobiotic exposure by increasing the activity of CYP450 and GST (García et al., 2005). For example, symbiodinium CYP enzymes were upregulated in response to thermal stress in the reef-building coral *Acropora millepora* as CYP450 hemoproteins are involved in cell detoxification and protection from oxidative stress (Rosic Nedeljka et al., 2010). The similar change of CYP450 and GST were also observed in the research of coral *P. damicornis* exposure to chlordecone. However, changes in the expression of CYP450 genes were also reported to be deleterious and high activities of CYP450 have been shown to induce carcinogens (Wecker et al., 2018). The pathways of organismal system were mostly related to immunity. For example, the upregulation of genes MASP1/2, C2, and Kallrein was found in the complement and coagulation cascades pathway, indicating that the host immune system was activated and currently suffering from pathogens or infections. MASPs are the enzymatic constituents of the lectin pathway of the complement system and are all potential targets of drug development. The upregulation of MASP1/2 gene indicated over activation of MASPs that may culminate into diseases. Some studies have shown that

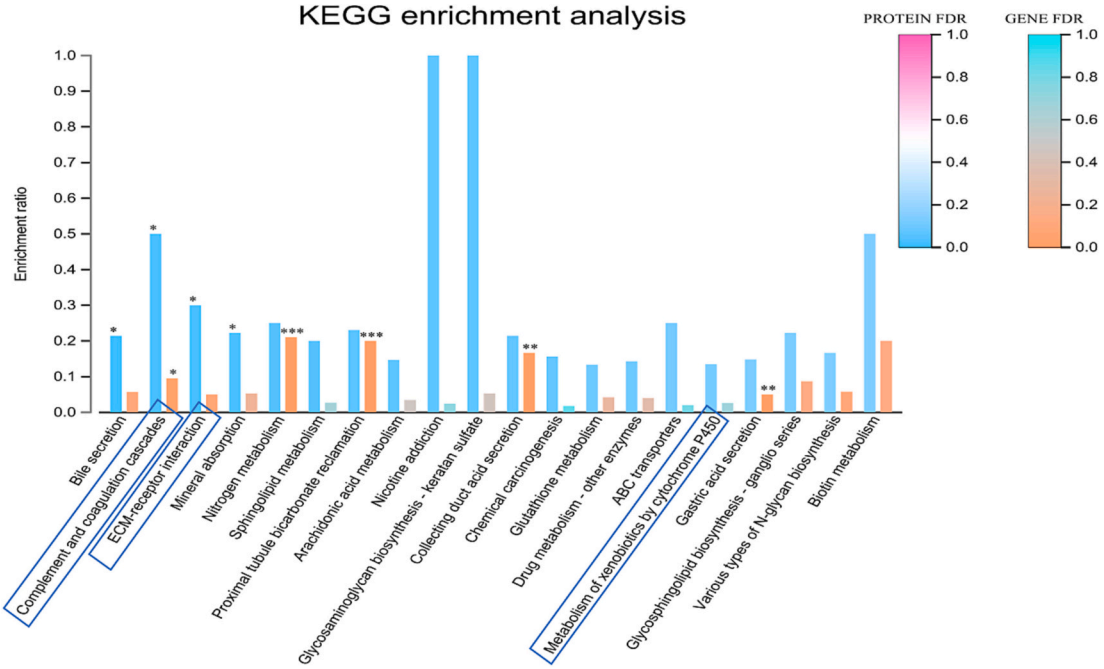

Fig. 6. Conjoint analysis of differentially expressed genes and proteins in the KEGG pathway of *P. lutea*.

the immune related genes and pathways including inflammatory response, antioxidant stress, and cell apoptosis may be activated when corals were subjected to environmental stress and pathogen infection (Wall et al., 2018). These immune-related pathways may overlap and interact with complement and coagulation cascade reactions, which is consistent with the conclusions of this study. Furthermore, the extracellular matrix (ECM) containing both proteins and polysaccharides plays important roles in cell adhesion, cell-cell interaction and cell communication between Symbiodiniaceae and host. The DEGs and DEPs associated with ECM-receptor interaction suggested that the ability of recognition and adhesion of *P. lutea* may be altered by PCP and confirmed the destruction of symbiotic relationship (Li et al., 2020b). The results all indicated that the host underwent a stress response of PCP exposure similar to the zooxanthellae. The immune system of the host was disrupted that could be linked to coral pathema prevalence which was consistent with the finding on the generation of pathogenic bacterium *Citrobacter*.

3.5. DEMs analysis of P. lutea under PCP exposure

The exchange of metabolites between stony corals, Symbiodiniaceae and associated microbes is the foundation of coral reef ecosystems (Boroujerdi et al., 2009). However, little about the metabolomic signatures of coral bleaching caused by chemical pollutants was known. The metaorganism was taken as the target rather than its individual components because metabolites were shared among all members of the coral holobiont. 85 upregulated and 19 downregulated differential metabolites (DEMs) were detected in the holobiont (Fig. S6). The DEMs involved in the functional pathways related to metabolism and organismal system derived from the joint analysis of transcriptome and proteomics were analyzed as shown in Fig. 7. It is worth noting that metabolite 1-naphthylamine (Fig. 7a) upregulated in the metabolism of xenobiotics by cytochrome P450 pathway. CYPs are a group of isoenzymes encoded by superfamily genes related to structure and function, mainly located in the endoplasmic reticulum, mitochondria and microsomes, which catalyze the metabolism of xenobiotics (Rosic Nedeljka et al., 2010). Aliphatic and aromatic compounds may be transformed into carcinogens by catalytic activation of CYPs such as 1-naphthylamine and its upregulation may cause coral diseases. Besides, phosphatidylcholines (PCs) are the key constituents of the bilayer, the variation of PCs may reflect the functional alteration of the cell membrane to affect the ability of cell proliferation. The upregulations of PC (18:1(9Z)/P-16:0) (Fig. 7b) in the arachidonic acid metabolism pathway suggested the membrane remodeling. The result was consistent with the metabolomics and lipidomics study on the impact of polybrominated diphenyl ether-47 on breast cancer mice and served as another evidence for pathema in coral *P. lutea* (Wei et al., 2020). Tryptophan and serotonin in the synaptic vesicle cycle were identified as DEMs in the pathways related to the organismal system. Tryptophan involved in oxidative respiration and energy metabolism is the main synthetic raw material of nicotinamide adenine dinucleotide (Wang et al., 2022). 5-hydroxytryptophan was produced by catalyzing of tryptophan by tryptophan hydroxylase and then catalyzed by 5-hydroxytryptophan decarboxylase to produce serotonin (Fig. 7c) which is an important substance that regulates neural activity. It was reported that exposure to the environmentally toxic pesticide maneb induced Parkinson's disease-like neurotoxicity in mice, the key factors in the tryptophan metabolism pathway including tryptophan and serotonin were decreased (Liu et al., 2022). However, PCP exposure upregulated the expression of both tryptophan and serotonin, possibly due to some biological tissues can release serotonin, which was pivotal in stress responses when subjected to certain chemical pollutants (Mustapha and Ji Ying, 2009).

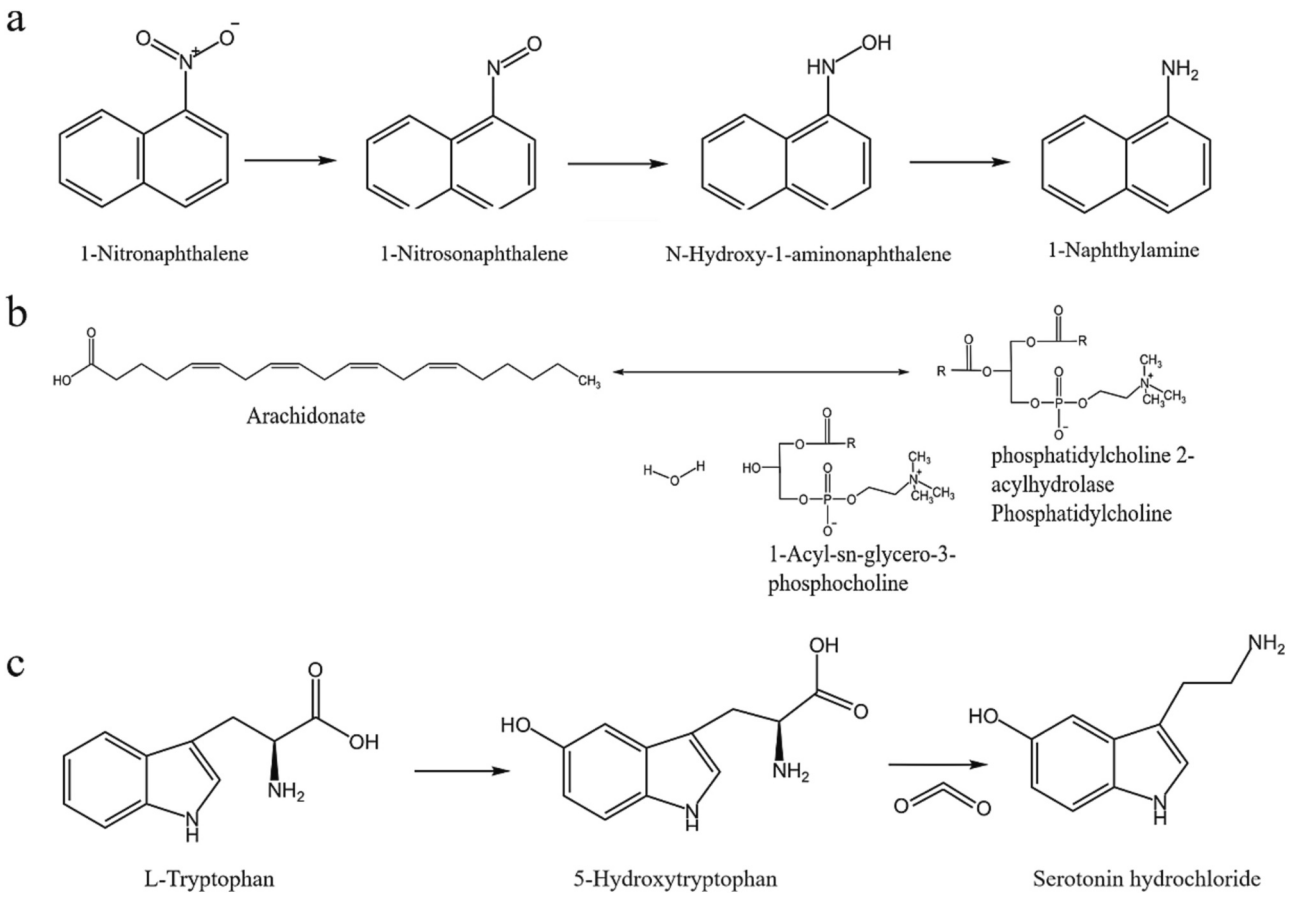

Fig. 7. Formation of DEMs of *P. lutea* related to metabolism and organismal system. (a) 1-Naphthylamine; (b) PC (18:1(9Z)/P-16:0); (c) Serotonin.

4. Conclusions

It was also proved that PCP could induce the expression of coral antioxidant enzymes. The increase of the pathogenic bacterium *Citrobacter* was confirmed to be one of the main stress responses of *P. lutea* to PCP stress and may also be one of the inducers of coral bleaching. In particular, the transcriptomics and proteomics results exhibited the disruptions of various biological functions of *P. lutea*, including the metabolism of amino acids and carbohydrates in zooxanthellae and the immune system of the host, etc. The upregulation of toxic metabolites such as 1-naphthylamine indicated that PCP induced coral pathema in *P. lutea*. Therefore, this study has important implications for further revealing the molecular mechanisms of coral pathema induced by PCP and provides a reference for the standard of PCP emissions of industrial pollutants along the coast.

CRediT authorship contribution statement

Yuanyuan Zhang: Investigation, Writing-Original draft preparation, Writing-Reviewing and Editing, Funding acquisition. **Lan Luo**: Writing-Original draft preparation, Experimental design and implementation and Editing, Data analysis. **Pin Gan, Xuan Chen, Xiaoli Li, Yan Pang**: Methodology, Experimental implementation. **Xiaopeng Yu**: Methodology, Data analysis. **Kefu Yu**: Conceptualization, Writing-review & editing. Validation, Funding acquisition.

Declaration of competing interest

The authors declare that they have no known competing financial interests or personal relationships that could have appeared to influence the work reported in this paper.

Data availability

Data will be made available on request.

Acknowledgements

This study was supported by the National Science Foundation China (No.42030502, No.42090041), the College Students' Innovative Entrepreneurial Training Plan Program (No.202310593494, No. 202310593257).

Appendix A. Supplementary data

Supplementary data to this article can be found online at https://doi.org/10.1016/j.scitotenv.2023.167956.

References

Ahasan, M.S., Picard, J., Elliott, L., Kinobe, R., Owens, L., Ariel, E., 2017. Evidence of antibiotic resistance in Enterobacteriales isolated from green sea turtles, Chelonia mydas on the Great Barrier Reef. Mar. Pollut. Bull. 120, 18–27. https://doi.org/10.1016/j.marpolbul.2017.04.046.

Beiras, R., Tato, T., 2018. Marine environmental risk assessment and acute water quality criterion for pentachlorophenol in coastal waters. Ecotoxicology 27, 803–808. https://doi.org/10.1007/s10646-018-1930-8.

Boroujerdi, A.F.B., Vizcaino, M.I., Meyers, A., Pollock, E.C., Huynh, S.L., Schock, T.B., et al., 2009. NMR-based microbial metabolomics and the temperature-dependent coral pathogen vibrio coralliilyticus. Environ. Sci. Technol. 43, 7658–7664. https://doi.org/10.1021/es901675w.

Chen, T., Li, S., Yu, K., Zheng, Z., Wang, L., Chen, T., 2013. Increasing temperature anomalies reduce coral growth in the Weizhou Island, northern South China Sea. Estuar. Coast. Shelf Sci. 130, 121–126. https://doi.org/10.1016/j.ecss.2013.05.009.

Chen, B., Yu, K., Liao, Z., Yu, X., Qin, Z., Liang, J., et al., 2021. Microbiome community and complexity indicate environmental gradient acclimatisation and potential microbial interaction of endemic coral holobionts in the South China Sea. Sci. Total Environ. 765, 142690 https://doi.org/10.1016/j.scitotenv.2020.142690.

Cheng, Y., Ekker, M., Chan, H.M., 2015. Relative developmental toxicities of pentachloroanisole and pentachlorophenol in a zebrafish model (Danio rerio). Ecotoxicol. Environ. Saf. 112, 7–14. https://doi.org/10.1016/j.ecoenv.2014.10.004.

Cheng, C.-M., Cheng, Y.-R., Ding, D.-S., Chen, Y.-T., Sun, W.-T., Pan, C.-H., 2021. Effects of ciliate infection on the activities of two antioxidant enzymes (SOD and CAT) in captive coral (Goniopora columna) and evaluation of drug therapy. Biology 10. https://doi.org/10.3390/biology10111216.

Chow, M.H., Tsang, R.H.L., Lam, E.K.Y., Ang, P., 2016. Quantifying the degree of coral bleaching using digital photographic technique. J. Exp. Mar. Biol. Ecol. 479, 60–68. https://doi.org/10.1016/j.jembe.2016.03.003.

Corinaldesi, C., Marcellini, F., Nepote, E., Damiani, E., Danovaro, R., 2018. Impact of inorganic UV filters contained in sunscreen products on tropical stony corals (Acropora spp.). Sci. Total Environ. 637-638, 1279–1285. https://doi.org/10.1016/j.scitotenv.2018.05.108.

Cunning, R., Gates, R.D., Edmunds, P.J., 2017. Using high-throughput sequencing of ITS2 to describe Symbiodinium metacommunities in St. John, US Virgin Islands. PeerJ 5, e3472. https://doi.org/10.7717/peerj.3472.

Danovaro, R., Bongiorni, L., Corinaldesi, C., Giovannelli, D., Damiani, E., Astolfi, P., et al., 2008. Sunscreens cause coral bleaching by promoting viral infections. Environ. Health Perspect. 116, 441–447. https://doi.org/10.1289/ehp.10966.

De Palmas, S., Denis, V., Ribas-Deulofeu, L., Loubeyres, M., Woo, S., Hwang, S.J., et al., 2015. Symbiodinium spp. associated with high-latitude scleractinian corals from Jeju Island, South Korea. Coral Reefs. 34, 919–925. https://doi.org/10.1007/s00338-015-1286-y.

Ding, J., Jiang, F., Li, J., Wang, Z., Sun, C., Wang, Z., et al., 2019. Microplastics in the Coral Reef Systems from Xisha Islands of South China Sea. Environ. Sci. Technol. 53, 8036–8046. https://doi.org/10.1021/acs.est.9b01452.

Drew, E.A., 1972. The biology and physiology of alga-invertebrates symbioses. II. The density of symbiotic algal cells in a number of hermatypic hard corals and alcyonarians from various depths. J. Exp. Mar. Biol. Ecol. 9, 71–75. https://doi.org/10.1016/0022-0981(72)90008-1.

Fel, J.-P., Lacherez, C., Bensetra, A., Mezzache, S., Béraud, E., Léonard, M., et al., 2018. Photochemical response of the scleractinian coral Stylophora pistillata to some sunscreen ingredients. Coral Reefs 38, 109–122. https://doi.org/10.1007/s00338-018-01759-4.

Feng, L., He, L., Jiang, S., Chen, J., Zhou, C., Qian, Z.J., et al., 2020. Investigating the composition and distribution of microplastics surface biofilms in coral areas. Chemosphere 252, 126565. https://doi.org/10.1016/j.chemosphere.2020.126565.

Feng, X., Sun, H., Liu, X., Zhu, B., Liang, W., Ruan, T., et al., 2022. Occurrence and ecological impact of chemical mixtures in a semiclosed sea by suspect screening analysis. Environ. Sci. Technol. 56, 10681–10690. https://doi.org/10.1021/acs.est.2c00966.

García, E., Ramos, R., Bastidas, C., 2005. Presence of cytochrome P450 in the Caribbean corals Siderastrea siderea and Montastraea faveolata. Cienc. Mar. 31, 23–30. https://doi.org/10.7773/cm.v31i11.81.

Han, M., Zhang, R., Yu, K., Li, A., Wang, Y., Huang, X., 2020. Polycyclic aromatic hydrocarbons (PAHs) in corals of the South China Sea: occurrence, distribution, bioaccumulation, and considerable role of coral mucus. J. Hazard. Mater. 384, 121299 https://doi.org/10.1016/j.jhazmat.2019.121299.

He, T., Tsui, M.M.P., Tan, C.J., Ma, C.Y., Yiu, S.K.F., Wang, L.H., et al., 2019. Toxicological effects of two organic ultraviolet filters and a related commercial sunscreen product in adult corals. Environ. Pollut. 245, 462–471. https://doi.org/10.1016/j.envpol.2018.11.029.

Helmkampf, M., Bellinger, M.R., Frazier, M., Takabayashi, M., 2019. Symbiont type and environmental factors affect transcriptome-wide gene expression in the coral Montipora capitata. Ecol. Evol. 9, 378–392. https://doi.org/10.1002/ece3.4756.

Hess, P., Altenhöfer, A., Khan, A.S., Daryab, N., Kim, K.S., Hacker, J., et al., 2004. A Salmonella fim homologue in Citrobacter freundii mediates invasion in vitro and crossing of the blood-brain barrier in the rat pup model. Infect. Immun. 72, 5298–5307. https://doi.org/10.1128/iai.72.9.5298-5307.2004.

Higuchi, T., Fujimura, H., Arakaki, T., Oomori, T., 2008. Activities of antioxidant enzymes (SOD and CAT) in the coral Galaxea fascicularis against increased hydrogen peroxide concentrations in seawater. In: Paper presented at the Proceedings of the 11th International Coral Reef Symposium.

Huang, W., Yang, E., Yu, K., Meng, L., Wang, Y., Liang, J., et al., 2022. Lower cold tolerance of tropical Porites lutea is possibly detrimental to its migration to relatively high latitude refuges in the South China Sea. Mol. Ecol. 31, 5339–5355. https://doi.org/10.1111/mec.16662.

Jiang, P., Wang, J., Sheng, N., Wei, D., Dai, J., 2017. Effects of pentachlorophenol on the quail (Coturnix japonica) liver detoxification pathway. Chemosphere 177, 44–50. https://doi.org/10.1016/j.chemosphere.2017.02.154.

Jiang, L., Sun, Y.F., Zhou, G.W., Tong, H.Y., Huang, L.T., Yu, X.L., et al., 2022. Ocean acidification elicits differential bleaching and gene expression patterns in larval reef coral Pocillopora damicornis under heat stress. Sci. Total Environ. 842, 156851 https://doi.org/10.1016/j.scitotenv.2022.156851.

Kobusińska, M.E., Witt, M., Lewandowski, K., Niemirycz, E., 2016. Partition of pentachlorophenol (PCP) into particulate and dissolved phases in the waters of the Vistula River mouth at the Gulf of Gdańsk. Oceanol. Hydrobiol. Stud. 45, 172–181. https://doi.org/10.1515/ohs-2016-0016.

Lewandowski, K.K., Cieslikiewicz, W., Kobusinska, M.E., Niemirycz, E., 2018. Sorption of pentachlorophenol (PCP) in the marine bottom sediments-batch sorption experiment at varying pressure. Environ. Sci. Pollut. Res. 25, 10799–10807. https://doi.org/10.1007/s11356-017-1076-x.

Lewis, S.E., Silburn, D.M., Kookana, R.S., Shaw, M., 2016. Pesticide behavior, fate, and effects in the tropics: an overview of the current state of knowledge. J. Agric. Food Chem. 64, 3917–3924. https://doi.org/10.1021/acs.jafc.6b01320.

Li, M., Liu, H., Guo, Y., Chen, F., Zi, X., Fan, R., et al., 2020a. Single symbiotic cell transcriptome sequencing of coral. Genomics 112, 5305–5312. https://doi.org/10.1016/j.ygeno.2020.10.019.

Li, T., Lin, X., Yu, L., Lin, S., Rodriguez, I.B., Ho, T.-Y., 2020b. RNA-seq profiling of Fugacium kawagutii reveals strong responses in metabolic processes and symbiosis potential to deficiencies of iron and other trace metals. Sci. Total Environ. 705, 135767 https://doi.org/10.1016/j.scitotenv.2019.135767.
Liang, J., Luo, W., Yu, K., Xu, Y., Chen, J., Deng, C., et al., 2022. Multi-omics revealing the response patterns of symbiotic microorganisms and host metabolism in Scleractinian coral Pavona minuta to temperature stresses. Metabolites 12. https://doi.org/10.3390/metabo12010018.
Liu, C., Liu, Z., Fang, Y., Du, Z., Yan, Z., Yuan, X., et al., 2022. Exposure to the environmentally toxic pesticide maneb induces Parkinson's disease-like neurotoxicity in mice: a combined proteomic and metabolomic analysis. Chemosphere 308, 136344. https://doi.org/10.1016/j.chemosphere.2022.136344.
Lohr, K.E., Khattri, R.B., Guingab-Cagmat, J., Camp, E.F., Merritt, M.E., Garrett, T.J., et al., 2019. Metabolomic profiles differ among unique genotypes of a threatened Caribbean coral. Sci. Rep. 9, 6067. https://doi.org/10.1038/s41598-019-42434-0.
Ma, Y., Li, T., Xia, H., Li, R., Cao, Y., Shi, H., et al., 2022. Effects of water masses and circulation on the surface water partial pressure of carbon dioxide in summer in eastern Beibu gulf, China. J. Mar. Sci. Eng. 11 https://doi.org/10.3390/jmse11010046.
Maheshwari, N., Khan, A.A., Ali, A., Mahmood, R., 2022. Oral administration of pentachlorophenol impairs antioxidant system, inhibits enzymes of brush border membrane, causes DNA damage and histological changes in rat intestine. Toxicol. Res. 11, 616–627. https://doi.org/10.1093/toxres/tfac035.
McCoshum, S.M., Schlarb, A.M., Baum, K.A., 2016. Direct and indirect effects of sunscreen exposure for reef biota. Hydrobiologia 776, 139–146. https://doi.org/10.1007/s10750-016-2746-2.
Michałowicz, J., Posmyk, M., Duda, W., 2009. Chlorophenols induce lipid peroxidation and change antioxidant parameters in the leaves of wheat (Triticum aestivum L.). J. Plant Physiol. 166, 559–568. https://doi.org/10.1016/j.jplph.2008.09.011.
Moraes, F.D., Rossi, P.A., Figueiredo, J.S.L., Venturini, F.P., Cortella, L.R.X., Moraes, G., 2016. Metabolic responses of channel catfish (Ictalurus punctatus) exposed to phenol and post-exposure recovery. An. Acad. Bras. Cienc. 88, 865–875. https://doi.org/10.1590/0001-3765201620150144.
Mustapha, M., Ji Ying, S., 2009. Intraflagellar transport/hedgehog-related signaling components couple sensory cilium morphology and serotonin biosynthesis in Caenorhabditis elegans. J. Neurosci. 29, 4065. https://doi.org/10.1523/JNEUROSCI.0044-09.2009.
Nahar, K., Baillie, J., Zulkarnain, N.A., 2023. Herbicide fate and transport in the great barrier reef: a review of critical parameters. Water 15. https://doi.org/10.3390/w15020237.
Nakamura, E., Yokohama, Y., Tanaka, J., 2004. Photosynthetic activity of a temperate coral Acropora pruinosa (Scleractinia, Anthozoa) with symbiotic algae in Japan. Phycol. Res. 52, 38–44. https://doi.org/10.1111/j.1440-1835.2004.tb00313.x.
Namit, A., Dowell, W., Matiasek, S., Webster, J., Stachura, D.L., 2022. Pentachlorophenol has significant adverse effects on hematopoietic and immune system development in zebrafish (Danio rerio). PloS One 17, e0265618. https://doi.org/10.1371/journal.pone.0265618.
Pei, J.Y., Yu, W.F., Zhang, J.J., Kuo, T.H., Chung, H.H., Hu, J.J., et al., 2022a. Mass spectrometry-based metabolomic signatures of coral bleaching under thermal stress. Anal. Bioanal. Chem. 414, 7635–7646. https://doi.org/10.1007/s00216-022-04294-y.
Pei, Y., Chen, S., Zhang, Y., Olga, V., Li, Y., Diao, X., et al., 2022b. Coral and it's symbionts responses to the typical global marine pollutant BaP by 4D-proteomics approach. Environ. Pollut. 307, 119440 https://doi.org/10.1016/j.envpol.2022.119440.
Pei, Y., Chen, S., Diao, X., Wang, X., Zhou, H., Li, Y., et al., 2023. Deciphering the disturbance mechanism of BaP on the symbiosis of Montipora digitata via 4D-proteomics approach. Chemosphere 312, 137223. https://doi.org/10.1016/j.chemosphere.2022.137223.
Pernice, M., Hughes, D.J., 2019. Forecasting global coral bleaching. Nat. Clim. Chang. 9, 803–804. https://doi.org/10.1038/s41558-019-0593-7.
Qin, Z., Yu, K., Chen, B., Wang, Y., Liang, J., Luo, W., et al., 2019. Diversity of Symbiodiniaceae in 15 coral species from the southern South China Sea: potential relationship with coral thermal adaptability. Front. Microbiol. 10, 2343. https://doi.org/10.3389/fmicb.2019.02343.
Raffa, R.B., Pergolizzi Jr., J.V., Taylor Jr., R., Kitzen, J.M., Group, N.R., 2019. Sunscreen bans: coral reefs and skin cancer. J. Clin. Pharm. Ther. 44, 134–139. https://doi.org/10.1111/jcpt.12778.
Reichert, J., Schellenberg, J., Schubert, P., Wilke, T., 2018. Responses of reef building corals to microplastic exposure. Environ. Pollut. 237, 955–960. https://doi.org/10.1016/j.envpol.2017.11.006.
Ritchie, R.J., 2006. Consistent sets of spectrophotometric chlorophyll equations for acetone, methanol and ethanol solvents. Photosynth. Res. 89, 27–41. https://doi.org/10.1007/s11120-006-9065-9.
Rosic Nedeljka, N., Pernice, M., Dunn, S., Dove, S., Hoegh-Guldberg, O., 2010. Differential regulation by heat stress of novel cytochrome P450 genes from the dinoflagellate symbionts of reef-building corals. Appl. Environ. Microbiol. 76, 2823–2829. https://doi.org/10.1128/AEM.02984-09.
Rougée, L., Downs, C.A., Richmond, R.H., Ostrander, G.K., 2006. Alteration of normal cellular profiles in the scleractinian coral (Pocillopora damicornis) following laboratory exposure to fuel oil. Environ. Toxicol. Chem. 25, 3181–3187. https://doi.org/10.1897/05-510R2.1.
Schreiber, U., 1986. Detection of rapid induction kinetics with a new type of high-frequency modulated chlorophyll fluorometer. Photosynth. Res. 9, 261–272. https://doi.org/10.1007/BF00029749.
Schwarz, J.A., Mitchelmore, C.L., Jones, R., O'Dea, A., Seymour, S., 2013. Exposure to copper induces oxidative and stress responses and DNA damage in the coral Montastraea franksi. Comp. Biochem. Physiol. C Toxicol. Pharmacol. 157, 272–279. https://doi.org/10.1016/j.cbpc.2012.12.003.
Shlesinger, T., van Woesik, R., 2023. Oceanic differences in coral-bleaching responses to marine heatwaves. Sci. Total Environ. 871, 162113 https://doi.org/10.1016/j.scitotenv.2023.162113.
Silva, D.P., Epstein, H.E., Vega Thurber, R.L., 2022. Best practices for generating and analyzing 16S rRNA amplicon data to track coral microbiome dynamics. Front. Microbiol. 13, 1007877. https://doi.org/10.3389/fmicb.2022.1007877.
Singh, S., Anand, R., 2023. Diverse strategies adopted by nature for regulating purine biosynthesis via fine-tuning of purine metabolic enzymes. Curr. Opin. Chem. Biol. 73, 102261 https://doi.org/10.1016/j.cbpa.2022.102261.
Sun, F., Yang, H., Zhang, X., Shi, Q., 2023. Metabolic and metatranscriptional characteristics of corals bleaching induced by the most severe marine heatwaves in the South China Sea. Sci. Total Environ. 858, 160019 https://doi.org/10.1016/j.scitotenv.2022.160019.
Takahashi, S., Murata, N., 2008. How do environmental stresses accelerate photoinhibition? Trends Plant Sci. 13, 178–182. https://doi.org/10.1016/j.tplants.2008.01.005.
Tang, J., Ni, X., Zhou, Z., Wang, L., Lin, S., 2018. Acute microplastic exposure raises stress response and suppresses detoxification and immune capacities in the scleractinian coral Pocillopora damicornis. Environ. Pollut. 243, 66–74. https://doi.org/10.1016/j.envpol.2018.08.045.
Thatje, S., 2021. Saving corals from bleaching. Environ. Sci. Technol. 55, 9634–9636. https://doi.org/10.1021/acs.est.1c03622.
Toonen, L.J.A., Overzier, M., Evers, M.M., Leon, L.G., van der Zeeuw, S.A.J., Mei, H., et al., 2018. Transcriptional profiling and biomarker identification reveal tissue specific effects of expanded ataxin-3 in a spinocerebellar ataxia type 3 mouse model. Mol. Neurodegener. 13, 31. https://doi.org/10.1186/s13024-018-0261-9.
Wall, C.B., Ricci, C.A., Foulds, G.E., Mydlarz, L.D., Gates, R.D., Putnam, H.M., 2018. The effects of environmental history and thermal stress on coral physiology and immunity. Mar. Biol. 165, 56. https://doi.org/10.1007/s00227-018-3317-z.
Wang, C., Qiu, J., Li, G., Wang, J., Liu, D., Chen, L., et al., 2022. Application and prospect of quasi-targeted metabolomics in age-related hearing loss. Hear. Res. 424, 108604 https://doi.org/10.1016/j.heares.2022.108604.
Watanabe, T., Yuyama, I., Yasumura, S., 2006. Toxicological effects of biocides on symbiotic and aposymbiotic juveniles of the hermatypic coral Acropora tenuis. J. Exp. Mar. Biol. Ecol. 339, 177–188. https://doi.org/10.1016/j.jembe.2006.07.020.
Wecker, P., Lecellier, G., Guibert, I., Zhou, Y., Bonnard, I., Berteaux-Lecellier, V., 2018. Exposure to the environmentally-persistent insecticide chlordecone induces detoxification genes and causes polyp bail-out in the coral P. damicornis. Chemosphere 195, 190–200. https://doi.org/10.1016/j.chemosphere.2017.12.048.
Wei, J., Li, X., Xiang, L., Song, Y., Liu, Y., Jiang, Y., et al., 2020. Metabolomics and lipidomics study unveils the impact of polybrominated diphenyl ether-47 on breast cancer mice. J. Hazard. Mater. 390, 121451 https://doi.org/10.1016/j.jhazmat.2019.121451.
Weis, V.M., 2008. Cellular mechanisms of Cnidarian bleaching: stress causes the collapse of symbiosis. J. Exp. Biol. 211, 3059–3066. https://doi.org/10.1242/jeb.009597.
Wright, R.M., Mera, H., Kenkel, C.D., Nayfa, M., Bay, L.K., Matz, M.V., 2019. Positive genetic associations among fitness traits support evolvability of a reef-building coral under multiple stressors. Glob. Change Biol. 25, 3294–3304. https://doi.org/10.1111/gcb.14764.
Xiang, N., Jiang, C.X., Huang, W., Nordhaus, I., Zhou, H.L., Drews, M., et al., 2019. The impact of acute benzo(a)pyrene on antioxidant enzyme and stress-related genes in tropical stony corals (Acropora spp.). Sci. Total Environ. 694 https://doi.org/10.1016/j.scitotenv.2019.07.280.
Xu, J., Chai, G., Xiao, Y., Xie, Z., Yang, X., Liao, B., et al., 2023. The community profiles of symbiotic bacteria at the different life stages of coral Dipsastraea favus. Front. Mar. Sci. 10 https://doi.org/10.3389/fmars.2023.1055848.
Yoshioka, Y., Yamashita, H., Suzuki, G., Zayasu, Y., Tada, I., Kanda, M., et al., 2021. Whole-genome transcriptome analyses of native symbionts reveal host coral genomic novelties for establishing coral-algae symbioses. Genome Biol. Evol. 13 https://doi.org/10.1093/gbe/evaa240.
Yu, W., Wang, W., Yu, K., Wang, Y., Huang, X., Huang, R., et al., 2019. Rapid decline of a relatively high latitude coral assemblage at Weizhou Island, northern South China Sea. Biodivers. Conserv. 28, 3925–3949. https://doi.org/10.1007/s10531-019-01858-w.
Yu, X., Yu, K., Huang, W., Liang, J., Qin, Z., Chen, B., et al., 2020. Thermal acclimation increases heat tolerance of the scleractinian coral Acropora pruinosa. Sci. Total Environ. 733, 139319 https://doi.org/10.1016/j.scitotenv.2020.139319.
Yu, X., Yu, K., Chen, B., Liao, Z., Liang, J., Yao, Q., et al., 2021a. Different responses of scleractinian coral Acropora pruinosa from Weizhou Island during extreme high temperature events. Coral Reefs. 40, 1697–1711. https://doi.org/10.1007/s00338-021-02182-y.
Yu, X., Yu, K., Liao, Z., Chen, B., Deng, C., Yu, J., et al., 2021b. Seasonal fluctuations in symbiotic bacteria and their role in environmental adaptation of the scleractinian coral Acropora pruinosa in high-latitude coral reef area of the South China Sea. Sci. Total Environ. 792, 148438 https://doi.org/10.1016/j.scitotenv.2021.148438.
Zhang, Y., Yang, Q., Zhang, Y., Ahmad, M., Ling, J., Tang, X., et al., 2021. Shifts in abundance and network complexity of coral bacteria in response to elevated ammonium stress. Sci. Total Environ. 768, 144631 https://doi.org/10.1016/j.scitotenv.2020.144631.
Zhang, Y., Chen, R.-W., Liu, X., Zhu, M., Li, Z., Wang, A., et al., 2022. Oxidative stress, apoptosis, and transcriptional responses in Acropora microphthalma under

simulated diving activities. Mar. Pollut. Bull. 183, 114084 https://doi.org/10.1016/j.marpolbul.2022.114084.
Zhang, Y., Huang, K., Chen, X., Wei, M., Yu, X., Su, H., et al., 2023. Inactivation of ciliate Uronema marinum under UV/peroxydisulfate advanced disinfection system in marine water. Sep. Purif. Technol. 305, 122563 https://doi.org/10.1016/j.seppur.2022.122563.
Zheng, W., Wang, X., Yu, H., Tao, X., Zhou, Y., Qu, W., 2011. Global trends and diversity in pentachlorophenol levels in the environment and in humans: a meta-analysis. Environ. Sci. Technol. 45, 4668–4675. https://doi.org/10.1021/es1043563.
Zheng, D., Jiao, H., Zhong, H., Qiu, J., Yan, X., Duan, Q., et al., 2018. Chlorophenols in marine organisms from the southern coast of Hangzhou Bay, China, and an assessment of risks posed to human health. J. Oceanol. Limnol. 36, 726–737. https://doi.org/10.1007/s00343-018-7039-3.